Mining Science, vol. 28, 2021, 233–245

www.miningscience.pwr.edu.pl

Mining Science

(Previously Prace Naukowe Instytutu Gornictwa Politechniki Wroclawskiej, ISSN 0370-0798)

ISSN 2300-9586 (print)
ISSN 2353-5423 (online)

Received January 19, 2021; Reviewed; Accepted September 24, 2021

INFLUENCE OF ADHESION ON STRESS–STRAIN CONDITION ALONGSIDE OF A FULL COLUMN RESIN CARTRIDGE ROCK BOLT

Ivan SAKHNO[1], Waldemar KORZENIOWSKI[2],
Kateryna SHEPTAK[2]*, Svitlana SAKHNO[1]

[1] Donetsk National Technical University, Ukraine
[2] AGH University of Science and Technology, Poland

Abstract: The article highlights the research pertaining to the problem of reinforcement of underground excavations with bolting system, using chemical method based on resin cartridges, which currently is a global trend in mines. Theoretical model of rock bolt installed in a rockmass was discussed and described with proper formulas for explanation the role of single discontinuity and its mechanism affecting stress–strain characteristics of the reinforcement system, based on an adhesive method. The presented model has been verified with results of numerical modelling of stress-strain and deformation composition of the "rock bolt/resin cartridge/rock block" system, depending on the bond coefficient of the mixture which fixes the rock bolt. The analysis of the modelling results showed that for the stress-strain conditions of the rock bolt, too high a bond between the bolt and the rock is dangerous (critical), as it leads to high local tensile and deformation stresses.

Keywords: *mine roadway, resin bolts, adhesion, stress–strain characteristics*

1. INTRODUCTION

Rock bolting is a widely used practice throughout the world to ensure stability of mining excavations (Cao et al. 2020; Hoien et al. 2021; Jahangir et al. 2021; Li 2020; Sakhno et al. 2018; Wu et al. 2021; Wen et al. 2016; Zhao et al. 2020). In practical mining applications rock bolts are fixed with mechanical expansion shell heads, chemical

* Corresponding author: Kateryna Sheptak (sheptak.kate@gmail.com)

doi: 10.37190/msc212817

(resin) cartridges and their adhesion properties, or as the result of frictional contact between the walls of the borehole and the bolt. The bolts of the first group are fixed in a borehole at “two points” – in the bottom part of the borehole and in the part of its outlet. The fastening quality of such a bolt and its load-bearing capacity are determined by the reliability of the locking element (head).

According to data from Li, Stjern and Myrvang (Li 2014), the load-bearing capacity of such bolts reach up to 160 kN with axial deformations of 55 mm, for bolts with a diameter of 20 mm. The disadvantage of this bolt group is its complexity of construction and assembling.

Bolts of the second group are installed with full length adhesion using resins, cement or other binding agents. According to Stillborg’s data for a 20 mm bolt, the load reaches 170 kN and 20 mm deformation, according to Stjern’s tests 210 kN and 40 mm, respectively (Li 2014). According to data of experiments by Skrzypkowski (Skrzypkowski 2021) tensile stress for partially embedded rock bolt over a distance of 0.3 m under load is more of 500 MPa. Rebar steel bolts, full column fixed, are the most widely used globally thanks to their priorities: simplicity, reliability, fast assembly. The disadvantage of this group of bolts is its delayed loading capacity. Laboratory tests (Li 2012) indicate that after a deformation of 20–30 mm based on 150 mm, such bolts are destroyed. This is due to the fact that a chemically fixed bolt is not able to deform along its entire length, which leads to its single point overload and destruction in and around the fracture deformation.

Friction bolts are fastened with frictional forces between the borehole walls and the bolt. This enables the formation of large deformations, but they have a much lower bearing capacity with pre-set constant resistance, as compared with the previously mentioned. According to tests conducted by Stillborg and Stjern for the Split Set bolts, the load-bearing capacity is about 50 kN with deformations of over 120 mm, and for the Swellex type bolt according to the tests, the maximum load-bearing capacity reaches 121 kN with deformations of 26 mm and after a 180 mm shift – 63 kN (Li 2014).

The most common are bolting systems in which the rods are fastened chemically, with the resin cartridges. Scientific research works on study of the stability of mining roadways, fixed with this type of bolts, mostly fails to into account the influence of the adhesion of binding mixtures with the bolt rod and the rock mass while the loading transfer. Contemporary studies, conducted mathematically, mainly by numerical methods, suggest the existence of a close connection between the bolt’s body and the rock block (Pruška 2017; Zesheng at al. 2016). As a rule, the rock bolt tests are focused on determining their physical characteristics (strength limits, liquid limit, etc.) or the rod profile (Ghadimi 2017; Li et al. 2016; Yokota et al. 2019). In this way, it is assumed that the role of the fastening structure is limited to ensuring that the bolt is securely fastened in the borehole. However, the study of dislocation spots in mining excavations, fastened with bolts, proves that often, even upon rock slide, bolting bolts remain intact, without any damage (Fig. 1). This means that a load-bearing component still has a margin of strength and the bolt/rock system does not work anymore since it is no longer optimized by stresses. In this way, the problem of the fastening system's reliability lies not only in the load-bearing element of the bolt system itself, but also in its interaction with the fastening element, the mode of operation of the fastening element and its characteristics. The importance of studying this problem is indicated by works Jahangir (Jahangir et al. 2021), Skrzypkowski (Skrzypkowski 2021), Wu (Wu et al. 2019).

a) b)

Fig. 1. Rock falls in mine roadway supported by rock bolts:
(a, b) Management Board of the "Pokrowskoje" mine, Ukraine (authors' photos)

The aim of the presented research was to determine the influence of the physical properties of the fastening system on the operation of the bolt/rock block system and the stress of its components. The basic property of the fastening component is the adhesion to the bolt rod.

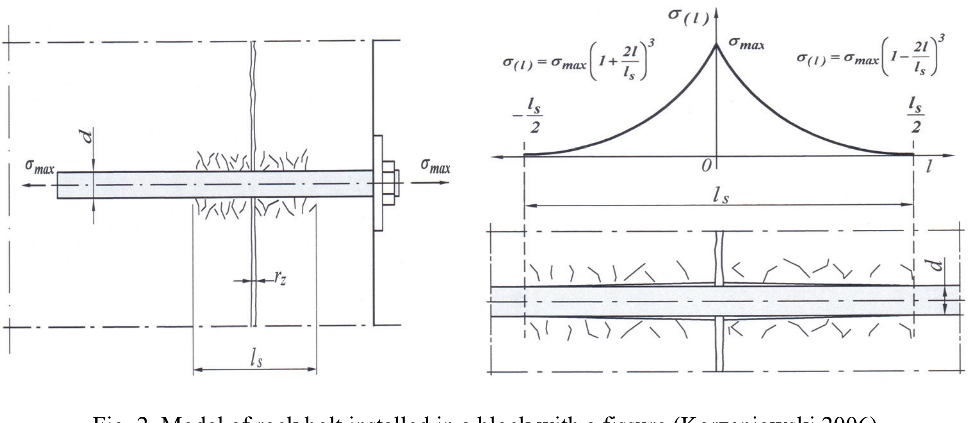

Fig. 2. Model of rock bolt installed in a block with a fissure (Korzeniowski 2006)

According to experience and findings of the authors (Korzeniowski 2006) in case of resin bolts installed especially in a laminated rock mass, a critical meaning for load bearing capacity of the bolting system has a plane of discontinuity (fissure) within the range of bolting zone. We assume that the rod subjected to the tension force firstly overcomes the adhesion forces adjoining the fissure r_z, at its both sides (Fig. 2).

Distribution of the tension stresses within the loaded bolt rod can be described with the formulas (1)–(5) within the range from $-l$ to 0, and from 0 to $+l$:

$$\sigma(l) = \sigma_{\max}\left(1 \pm \frac{2l}{l_s}\right)^3 \quad \text{or} \quad F_{st}(l) = F_{st\,kr}\left(1 \pm \frac{2l}{l_s}\right)^3, \tag{1}$$

where:

$\sigma_{\max}$ – maximum stress along the loading force direction,

l – current coordinate along the length of the rod,

l_s – length of the rod adjoining the fissure, separated from the binding compound.

Beside of the tension stresses in the loaded bolt shear stresses are induced at the rock/binding compound/rod contacts, responsible for the final load bearing capacity. Assuming the boundary condition for shearing of the contacts of the rod with φ perimeter and the cross-section are s we can write a formula:

$$\tau(l) \cdot \varphi \cdot dl = s \cdot d \cdot \sigma(l) \tag{2}$$

and after transformation we obtain:

$$\tau(l) = \frac{s}{\varphi} \cdot \frac{d\sigma(l)}{dl}. \tag{3}$$

Putting value $\sigma(l)$ from formula (1) and differentiation according l we get:

$$\tau(l) = \frac{s}{\varphi} \cdot \left[\frac{6 \cdot \sigma_{\max}}{l_s}\left(1 + \frac{2 \cdot l}{l_s}\right)^2\right]. \tag{4}$$

Within the range from $-l$ to 0 (one side of the fissure) we obtain, and within the range from 0 to $+l$ (the other side of the fissure):

$$\tau(l)_{-l \to 0\,(0 \to +l)} = \pm \frac{6 \cdot s}{\varphi \cdot l_s} \cdot \sigma_{\max}\left(1 \pm \frac{2 \cdot l}{l_s}\right)^2. \tag{5}$$

For $l = 0$, $\tau(l)_{\max}$ is described as following:

$$\tau_{\max} = \pm \frac{6 \cdot s}{\varphi \cdot l_s} \cdot \sigma_{\max}. \tag{6}$$

2. NUMERICAL MODELLING

Numerical modelling was used as a method of analysis, carried out in volumetric on a natural scale with the use of FEM simulation with ANSYS.

A section of a rock block, represented by sand slate, was modelled and a borehole with a diameter of 40 mm and a depth of 2.0 m was drilled in it, where the steel bolt of 30 mm in diameter was fixed in. The space between the borehole walls and the bolt body was filled with a binding compound. It was assumed that the modelled block was split, which causes one of its parts to move towards the excavation. Stresses which caused the displacement of the block in the model were inflated on the surface of the cross-section of the rock; they were gradually increased to feasible limits. Through the symmetry of the tasked axis, half of the cross-sectional area of the system was modelled (Fig. 3). The task was solved with an elastic non-linear set-up; the system had two contact surfaces. The first one between the bolt body and the fastening structure, the second one between the binding and the rock block.

Since the bonding mixture is homogeneous, the difference between adhesion to metal and rock is constant. In the finite element model, the adhesion was determined by the friction coefficient. Correspondingly, the lower threshold of adhesion was the dry friction coefficient. For the connecting pair metal/coupling composition, the coefficient was 0.45, and for the pair coupling composition/rock, it was 0.6.

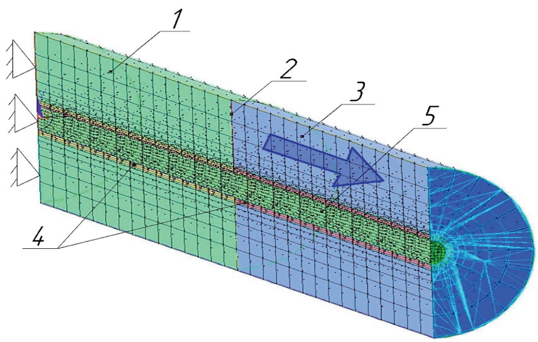

Fig. 3. General view of the finite element model:
1 – fixed part of block, 2 – tearing fracture, 3 – detached part of block,
4 – fastening structure; 5 – rock bolt

The difference in the rate of adhesion between the pairs was 0.15 units. Bolt rods are usually made of armature steel, which significantly increases the actual connection between the bolt body and the connecting compound. Therefore, a more interesting and indicative value for the study is the size of the bond in the contact pair coupling composition-rock. While modelling, this parameter ranged from 0.6–10 units.

3. RESULTS AND DISCUSSION

Images of the distribution of von Mises equivalent stresses and deformations in the model at 1 MPa of pressure on the detaching part of the block and 0.6 and 10 unit rock interface sizes are shown in Fig. 4.

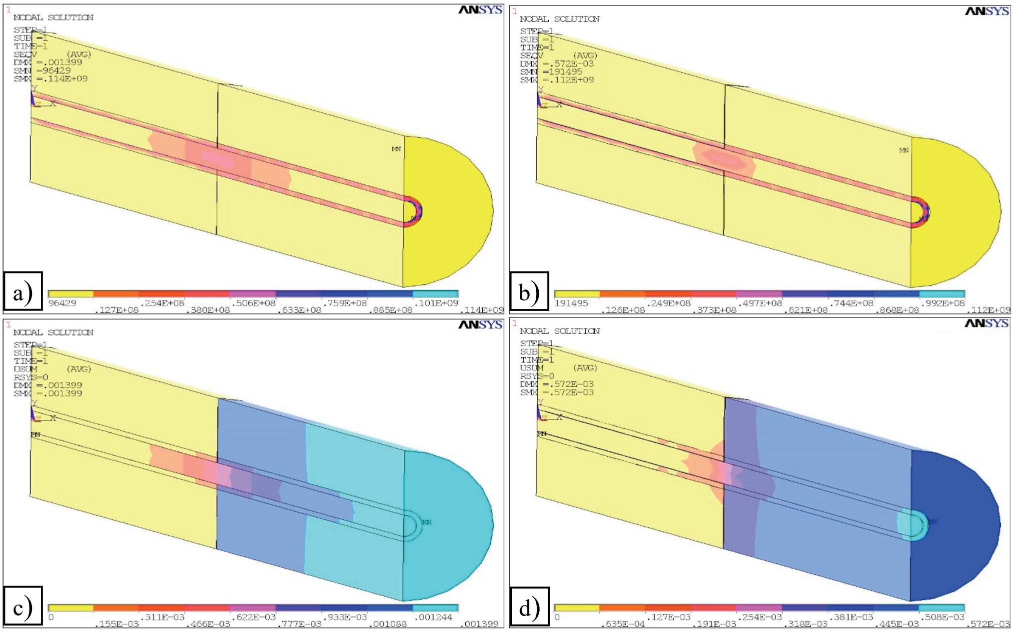

Fig. 4. Distribution of von Mises equivalent stresses (a, b) and total displacements in the model (c, d) with a bond of 0.6 (a, c) and 10 (b, d) units

The presented results show that the bolt stress is local with the maximum stress corresponding to the tearing fracture. With a binding equal to 10 the displacement of the block is 2.45 times lower than with a binding equal to 0.6. The coupling compound is loaded over the entire length of the hole with a maximum stress at the fracture boundary. Only the part of the bonding mixture at the block boundary is deformed. No additional stress is created in the rock blocks themselves.

In order to evaluate the influence of the tested parameters on the composition of the system's components, we will analyse the deformations and stresses occurring in a critical cross-sections, reducing them to graphs of projections constructed according to characteristic lines. Line 1-1 coincides with the central longitudinal axis of the bolt and characterises the bolt beam. Line 2-2 is parallel to the first one, but it was drawn on the connection boundary between the composition and the rock, thus determining its condition. Line 3-3 approximates the first one, but it was drawn through the centres of the rock blocks. The lines and points for determining deformation and stress are shown Table 1.

Table 1. Point coordinates by line

Points	Coordinates (*x*; *y*; *z*) on characteristic lines			Points	Coordinates (*x*; *y*; *z*) on characteristic lines		
	Line 1-1	Line 2-2	Line 3-3		Line 1-1	Line 2-2	Line 3-3
1	(0; 0; 0)	(0; 0.02; 0)	(0; 0.055; 0)	11	(0; 0; 1.0)	(0; 0.02; 1.0)	(0; 0.055; 1.0)
2	(0; 0; 0.15)	(0; 0.02; 0.15	(0; 0.055; 0.15	12	(0; 0; 1.05)	(0; 0.02; 1.05)	(0; 0.055; 1.05)
3	(0; 0; 0.3)	(0; 0.02; 0.3	(0; 0.055; 0.3	13	(0; 0; 1.1)	(0; 0.02; 1.1)	(0; 0.055; 1.1)
4	(0; 0; 0.4)	(0; 0.02; 0.4	(0; 0.055; 0.4	14	(0; 0; 1.2)	(0; 0.2; 1.2)	(0; 0.055; 1.2)
5	(0; 0; 0.5)	(0; 0.02; 0.5	(0; 0.055; 0.5	15	(0; 0; 1.3)	(0; 0.02; 1.3)	(0; 0.055; 1.3)
6	(0; 0; 0.6)	(0; 0.02; 0.6)	(0; 0.055; 0.6)	16	(0; 0; 1.4)	(0; 0.02; 1.4)	(0; 0.055; 1.4)
7	(0; 0; 0.7)	(0; 0.02; 0.7)	(0; 0.055; 0.7)	17	(0; 0; 1.55)	(0; 0.02; 1.55)	(0; 0.055; 1.55)
8	(0; 0; 0.8)	(0; 0.02; 0.8)	(0; 0.055; 0.8)	18	(0; 0; 1.7)	(0; 0.02; 1.7)	(0; 0.055; 1.7)
9	(0; 0; 0.9)	(0; 0.02; 0.9)	(0; 0.055; 0.9)	19	(0; 0; 1.85)	(0; 0.02; 1.85)	(0; 0.055; 1.85)
10	(0; 0; 0.95)	(0; 0.02; 0.95)	(0; 0.055; 0.95)	20	(0; 0; 2.0)	(0; 0.02; 2.0)	(0; 0.055; 2.0)

Deformations in the block fastened with the bolt are caused by displacement of its detached part; it is convenient to analyse it by drawing appropriate structures along line 3-3. The diagrams presenting the characteristics of rock block deformations at 1 MPa pressure on the detaching part of the rock (Fig. 5) make it possible to conclude that increased binding leads to a reduction of the detaching block.

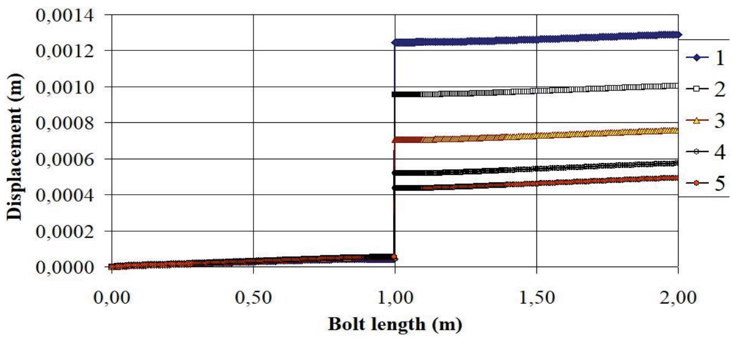

Fig. 5. Longitudinal deformations of rock blocks (line 3-3) at 1 MPa pressure on the detaching part of the block at the rock interface:
1 – 0.6 units; 2 – 1 units; 3 – 2 units; 4 – 5 units; 5 – 10 units

The quantitative evaluation of the impact of the binding on the stress and deformation condition of the bolt rod in the model under analysis is presented in diagrams (Figs. 6 and 7).

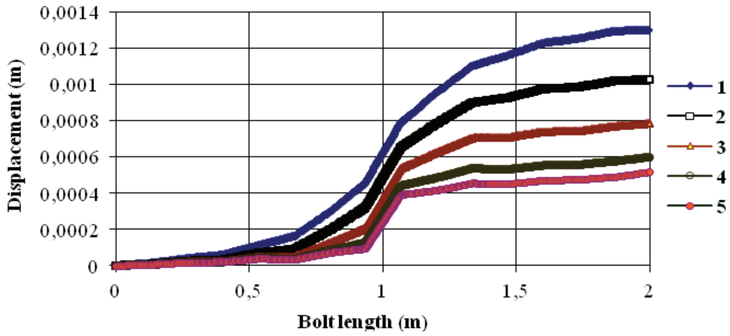

Fig. 6. Bolt rod's deformations along length (line 1-1) at 1 MPa pressure on the detaching part of the block, at rock interface: 1 – 0.6 unit; 2 – 1 unit; 3 – 2 units; 4 – 5 units; 5 – 10 units

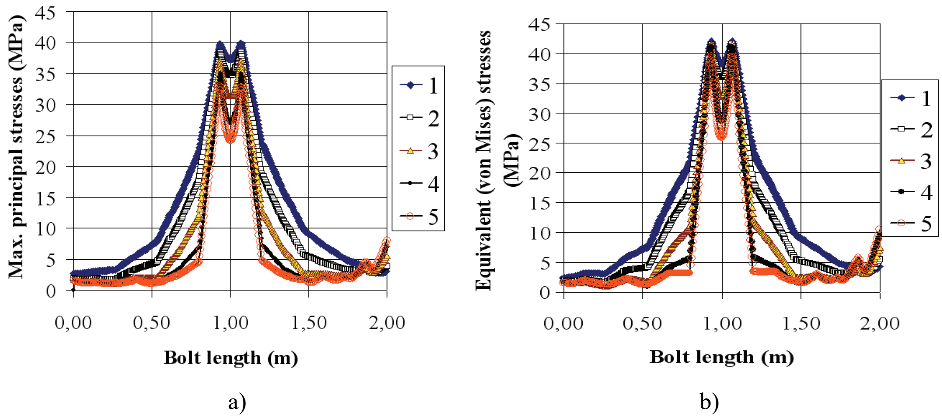

Fig. 7. Maximum major stresses (a) occurring and maximum (von Mises) equivalent stresses (b) in the bolting beam along its length (line 1-1) at 1 MPa pressure on the detaching part of the block, at rock interface: 1 – 0.6 unit; 2 – 1 unit; 3 – 2 units; 4 – 5 units; 5 – 10 units

The largest part of the deformation diagrams corresponds to the middle part of the bolt and lies within the rage of 0.95–1.05 m. At the same time, it is worth noting that, as binding increases, the general deformations of the bolt decrease and there is no deformation in the specified region. In order to follow this, we will analyse the diagrams of relative deformations of the bolt beam between neighbouring points placed in the appropriate positions (Fig. 8). Figure 8a shows that, as binding increases, the general deformations of the bolt decrease and deformation increases at section 0.95–1.05. It means that improving the quality of the bolt fastening mechanism leads to an increase in its local relative deformations, which is more critical. In the former case, the entire bolt rod stretches continuously and, in the latter one, only the middle part stretches more significantly, where higher stresses appear. It can be also observed on the basis of stress diagrams. Two stress increases are observed in the middle part of the bolt. The first one, at section 0.8–0.95 m, 1.05–1.2 where binding leads to an increase in stress growth (increase). For the 0.6 unit binding, the principal stresses at this section increase 1.76 times and, for binding 10, 7.26 times. Another pressure increase is observed in the middle part of the bolt beam at section 0.95–1.05 m. At this section, the increase in binding also leads to an increase in the difference between maximum stresses; for the 0.6 unit binding, the principal stresses at this section decrease 1.06 times and, for binding 10, 1.34 times. It is thus obvious to conclude that high binding is more dangerous for the stress and deformation condition of the bolt beam since it leads to the occurrence of higher local stresses and deformations. It is necessary to pay attention to the fact that relative deformations of the bolt rod are irregular at length and unsymmetrical, which is more visible as stress on the displacing rock block increases (Fig. 8b).

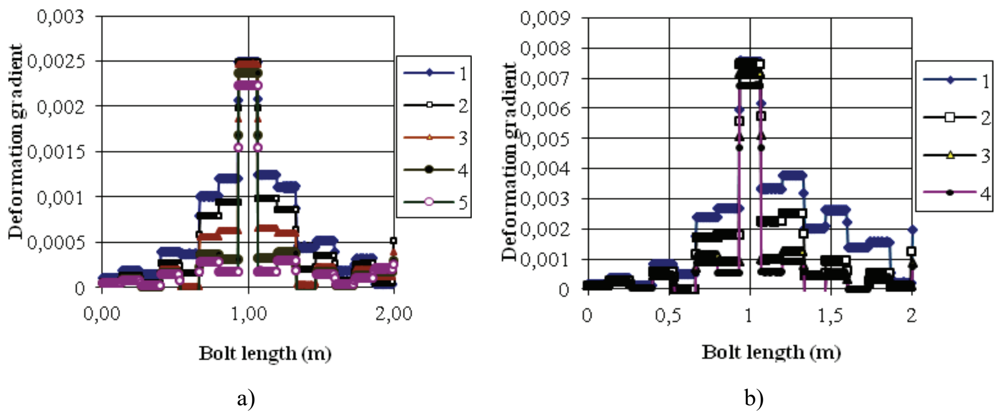

Fig. 8. Relative deformations of the bolting beam along its length (line 1-1) at 1 MPa (a) and at 3 MPa (b) pressure on the detaching part of the block, at rock interface: 1 – 0.6 unit; 2 – 1 unit; 3 – 2 units; 4 – 5 units; 5 – 10 units

The diagrams show that, at binding exceeding 5 units, relative deformations are a constant. Until this moment, an increase in deformations is observed relative to the bond coefficient, which is approximate to a logarithmic one. In order to observe the impact of bonding on the deformation of the coupling composition in the under analysis, it is necessary to analyse the relevant diagrams (Fig. 9).

The basic difference between the deformation of the fastening element and the deformation of the bolt rod consists in the existence of a displacement increase in the zone between longitudinal blocks. In addition to this, displacements do not differ significantly in the immobile part of the block at different bond coefficients. The higher the bond, the worse the deformation curve of the displacing block.

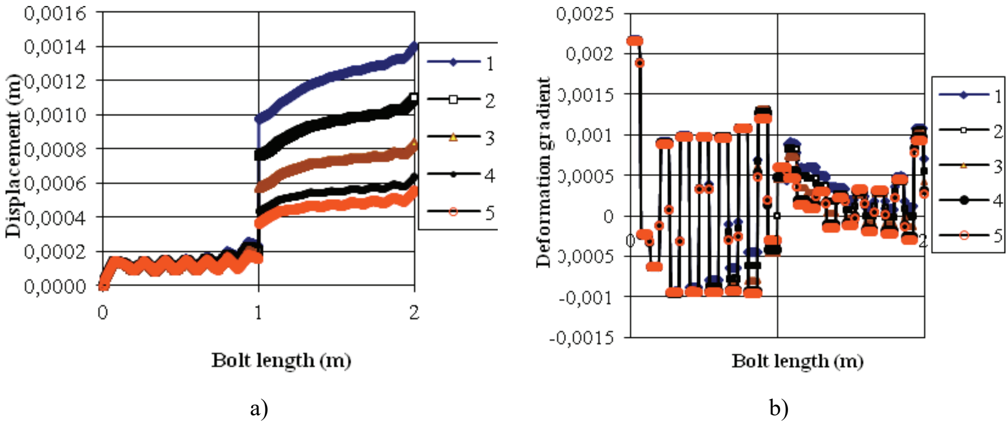

Fig. 9 – Deformations (a) and relative deformations (b)
of the binding compound along its length (line 2-2) at 1 MPa pressure
on the detaching part of the block, at rock interface:
1 – 0.6 unit; 2 – 1 unit; 3 – 2 units; 4 – 5 units; 5 – 10 units

When analysing the equivalent stresses (Fig. 10a), one can reach a similar conclusion. The stresses show an irregular distribution along the length with increased amplitude towards the detaching block. Increased stress in the section dangerous for the bolt beam 0.95–1.05 m constitutes 20–26% of the stress at adjacent sections.

While tensile strain is critical for the bolt rod, compressive strain is dangerous for the fastening structure. This is shown in the diagrams of main stress (Fig. 10b) occurring at its length. For the presented example, minimum (compressing) principal stresses are 74.6 MPa and the maximum ones are also compressing and equal to 6.6 MPa. It is obvious that minimum principal stresses which grow as the coupling coefficient increases are also dangerous for the structure.

The occurrence of high stresses in the anchor bolt and even the danger of its destruction with resins with high adhesion are confirmed by laboratory experiments under the guidance of Prof Korzeniowski (Skrzypkowski et al. 2020). The presented results of numerical modelling in terms of the effect of the elastic modulus of the resin on the nature of stresses and failures arising in it are consistent with the results of laboratory tests of the effect of resin properties on the peak pullout forces mentioned in the work of Shen (Shen 2021), as well as in the works of Sakhno (Sakhno et al. 2018; Sakhno et al. 2019).

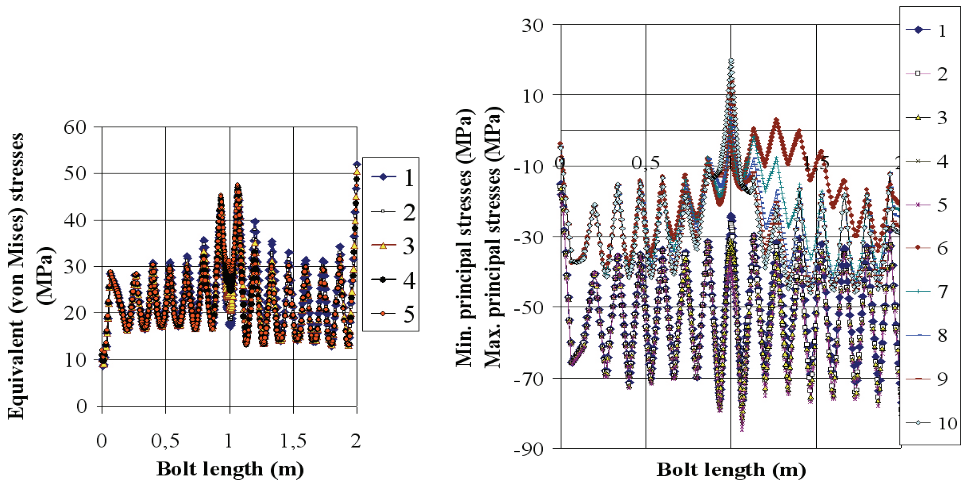

a) b)

Fig. 10. Von Mises equivalent stresses (a) and principal stresses (b) occurring in the fastening structure along its length (line 2-2) at 1 MPa pressure on the detaching part of the block, at rock interface: (for 17a) 1 – 0.6 unit; 2 – 1 unit; 3 – 2 units; 4 – 5 units; 5 – 10 units; (for 17b) 1-5 minimum principal stresses (S_3) at rock interface: 1 – 0.6 unit; 2 – 1 unit; 3 – 2 units; 4 – 5 units; 5 – 10 units; 6–10 maximum principal stresses (S_1) at rock interface: 6 – 0.6 unit; 7 – 1 unit; 8 – 2 units; 9 – 5 units; 10 – 10 units

4. CONCLUSIONS

Based on the results achieved, the following conclusions can be drawn:

1) As the bond increases, main deformations of the bolt decrease and relative deformations near the detaching fracture grow based on an approximately logarithmic relationship of the connection coefficient.
2) Relative deformations of the coupled composition in the middle part of the system "rock/bolt/resin", near the fracture, are 2 times lower than in case of the bolt rod and, at the same time, they are quite uniform.
3) Stresses in the coupled fastening structure are distributed in an irregular manner at length with amplitude increasing towards the detaching block. The increase of stress in the section critical for the bolt rod constitutes 20–26% of stress at adjacent sections. Minimum principal stresses which grow as the connection coefficient increases are critical.
4) For the stress and deformation condition of the bolt rod, the strong coupling of the bolt and the rock is more dangerous since it leads to occurrence of higher local tensile stress and deformation. The occurring stresses specify the necessary material and diameter of the bolt rod.

This article has been financed from AGH University of Science and Technology, Cracow, Poland, and statuary research fund: 11.11.100.005 and 15.11.100.073.

REFERENCES

CAO J., ZHANG N., WANG S., QIANA D., XIEA Z., 2020, *Physical model test study on support of super pre-stressed anchor in the mining engineering*, Engineering Failure Analysis, 118, 104833.

GHADIMI M., 2017, *Effect of profile bolt in bond strength fully grouted rock bolts using analytical andexperimental methods*, International Journal of Mining and Mineral Engineering, Vol. 8, Issue 2, 156–168.

HOIEN A.H., LI C.C., ZHANG N., 2021, *Pull-out and Critical Embedment Length of Grouted Rebar Rock Bolts-Mechanisms when Approaching and Reaching the Ultimate Load*, Rock Mechanics and Rock Engineering, 54, 1–18.

JAHANGIR E., BLANCO-MARTÍN L., HADJ-HASSEN F., TIJANI M., 2021, *Development and application of an interface constitutive model for fully grouted rock-bolts and cable-bolts*, Journal of Rock Mechanics and Geotechnical Engineering, 13 (4), 811–819; https://doi.org/10.1016/j.jrmge.2021.03.011

KORZENIOWSKI W., 2006, *Evaluation of State of Underground Gateroads and Rooms Based on Empirical Research Method*, Wydawnictwo AGH University of Science and Technology, Monographs, ISSN 0867-6631, Cracow.

LI C., 2012, *Performance of D-bolts Under Static Loading*, Rock Mechanics and Rock Engineering, 45 (2), 183–192.

LI C.C., 2020, *Principles and methods of rock support for rock burst control*, Journal of Rock Mechanics and Geotechnical Engineering, 12, 1–14.

LI C., STJERN G., MYRVANG A., 2014, *A review on the performance of conventional and energy-absorbing rockbolts*, Journal of Rock Mechanics and Geotechnical Engineering, 6, 315–327.

LI L., HAGAN P., SAYDAM S., HEBBLEWHITE B., 2016, *Shear resistance contribution of support systems in double shear test*, Tunnelling and Underground Space Technology, 56, 168–175.

PRUŠKA J., 2017, *Modelling rock mass improvement using rock bolts*, Acta Polytechnica CTU Proceedings, 10, 43–47.

SAKHNO I., SAKHNO, S., ISAIENKOV O., Kurdiumow D., 2019, *Laboratory studies of a high-strength roof bolting by means of self-extending mixtures*, Mining of Mineral Deposits, 13 (2), 17–26.

SAKHNO I., SAKHNO S., KURDIUMOW D., SHVETS I., 2018, *Studies of new nonadhesive anchoring*, Mining of Mineral Deposits, Vol. 12, Issue 2, 85–94.

SHEN J., 2021, *Experimental study on anchorage performance of resin grout with steel segment*, Advances in Civil Engineering, Vol. Article ID 5580555, 19 pp.

SKRZYPKOWSKI K., 2021, *An Experimental Investigation into the Stress–Strain Characteristic under Static and Quasi-Static Loading for Partially Embedded Rock Bolts*, Energies, 14, 1483.

SKRZYPKOWSKI K., KORZENIOWSKI W., ZAGÓRSKI K., ZAGÓRSKA A., 2020, *Modified rock bolt support for mining method with controlled roof bending*, Energies, Vol. 13, No. 8, pp. 1–20.

WEN Z., JIANG Y., HAN Z, YANG S., WANG X., 2016, *Bolting Principles of a New Energy-Absorbing Expandable Rock Bolt*, Engineering Transactions, Vol. 64, Issue 1, 89–103.

WU K., SHAO Z.S., QIN S., WEI W., CHU Z., 2021, *A critical review on the performance of yielding supports in squeezing tunnels*, Tunn. Undergr. Space Technol., Vol. 114, 103815.

WU X., JIANG Y., WANG G., GONG B., GUAN Z., DENG T., 2019, *Performance of a New Yielding Rock Bolt Under Pull and Shear Loading Conditions*, Rock Mechanics and Rock Engineering, 52, 3401–3412.

YOKOTA Y., ZHAO Z., SHANGA J., NIE W., DATE K., IWANO K., OKADA Y., 2019, *Effect of bolt configuration on the interface behaviour between a rock bolt and bond material: A comprehensive DDA investigation*, Computers and Geotechnics, 105, 116–128.

ZHAO X., ZHANG S., ZHU Q., LI H., CHEN G., ZHANG P., 2020, *Dynamic and static analysis of a kind of novel J energy-releasing bolts*, Geomatics. Natural. Hazards Risk, Vol. 11, 2486–2508.

ZESHENG D., BOTAO Q., FUCHAO T., 2016, *Numerical analysis of the effects of rock bolts on stress redistribution around a roadway*, International Journal of Mining Science and Technology, 26 (6), 975–980.